Desalinating young sea ice enhances turbulent ocean heat flux

Algot K. Peterson[1,2]

[1]University of Bergen, Norway

[2]Bjerknes Centre for Climate Research, Norway

Key Points:

- Unprecedented observations of saline plumes descending from drifting Arctic sea ice.
- Accumulated salt flux corresponds to observed salt reduction between two nearby ice cores.
- Desalination processes may be of increasing importance with an increasing fraction of first year ice.

Corresponding author: Algot K. Peterson, `algot@uib.no`

Abstract

In sea ice, interconnected pockets and channels of brine are surrounded by fresh ice. Over time, brine is lost by gravity drainage and flushing. The timing of salt release and its interaction with the underlying water can have great impact on sea ice melt. Unprecedented observations of salty plumes descending from drifting Arctic sea ice are presented here. The plumes are likely triggered by oceanic heat through bottom melt when the ice is sufficiently warm and permeable. The average oceanic heat flux is 1058 W m^{-2} for 131 identified plumes lasting a total of 31 minutes. The plumes observed here contribute ~5 W m^{-2} directly to observed average heat fluxes, alter the distribution of salinity in the surface layer and could also affect stability. The total observed salt flux accumulates to 7.6 kg m^{-2}, and compares well with the salt reduction found between two nearby ice cores. The increasing fraction of younger, more saline ice in the Arctic suggests the impact of desalination processes is increasing with the transition to the 'new Arctic'.

1 Introduction

In the Arctic Ocean, sea ice is an effective barrier for exchange between the ocean and atmosphere. The presence of sea ice is, however, depending on a delicate balance between the atmospheric and oceanic heat fluxes. The inflowing Atlantic water contains enough heat to melt the Arctic sea ice in a few years [*Turner*, 2010], and a small change in oceanic heat flux can have huge implications for the heat balance at the interface. Understanding the processes that control vertical heat fluxes under the sea ice is important to understand the response of sea ice to a changing climate [*Carmack et al.*, 2015]. The interplay between heat and salt exchange at the ice-ocean interface can work to enhance or reduce sea ice melt in the Arctic Ocean [*Sirevaag*, 2009].

While sea ice in bulk is a source of fresh water to the upper ocean, the sea ice consists of fresh ice surrounding pockets of liquid brine, connected through a network of channels and capillaries [*Petrich and Eicken*, 2010]. The brine remains at its salinity-determined freezing point, in thermal equilibrium with the surrounding ice, and brine salinity and volume adjusts to temperature changes by growing or melting fresh ice.

Over time, salt is lost from the sea ice. Timing of the salt release and how the salt is distributed in the water column is important in the evolution of the Arctic mixed layer. The main desalination processes of sea ice are gravity drainage and flushing of melt ponds [*Notz*

and Worster, 2009]. While melt ponds are present only in advanced stages of melt, gravity drainage occurs throughout the seasons. Ice permeability is a controlling factor for gravity drainage, increasing with temperature as the ice warms [*Golden et al.*, 1998]. When sea ice warms to within a certain critical temperature range, full depth brine convection and desalination can occur, even before the onset of melt [*Jardon et al.*, 2013]. Furthermore, gravity drainage has been successfully modeled using a 1D sea ice model, and can be triggered both by atmospheric heat and bottom melt from oceanic heat [*Griewank and Notz*, 2013].

Despite theoretical understanding and successful modeling of spring-time brine convection, observations are sparse. Brine drainage in response to atmospheric warming may have been the cause of observed salinity anomalies below sea ice in Storfjorden [*Jardon et al.*, 2013]. Still, the main evidence so far has been observations of saline plumes descending from warming landfast sea ice in a Svalbard fjord [*Widell et al.*, 2006]. It has been hypothesized that this form of desalination can occur on drifting Arctic sea ice, but so far this has remained unverified. The existence of such plumes can be of great importance to the release of salt from ice, its subsequent distribution in the upper water column, and could thus weaken the otherwise strong surface stratification typical below melting ice.

The first observations of brine plumes released from drifting sea ice in the Arctic Ocean are presented here. The observations are collected in June 2015, in the MIZ north of Svalbard. The data is a subset of a previously reported under-ice turbulence data set [*Peterson et al.*, 2017, 2016], and is part of the Norwegian Young Sea Ice Cruise (N-ICE2015) [*Granskog et al.*, 2016].

2 Data and methods

2.1 Turbulence instrument cluster

Under-ice turbulence measurements were made using a turbulence instrument cluster (TIC) deployed 1 m below the ice undersurface, relying on eddy-covariance to calculate turbulent fluxes of momentum and scalars from point measurements of temperature, salinity and currents. The concept is well-proven, and processing follows previous studies [*McPhee*, 2002; *McPhee et al.*, 2008]. Detailed description of the setup is given in *Peterson et al.* [2017], briefly summarized below. Horizontal and vertical currents are rotated into the mean current direction (u), such that cross-stream (v) and vertical (w) current averages zero for a given 15-minute segment. Each segment is subject to an extensive quality control,

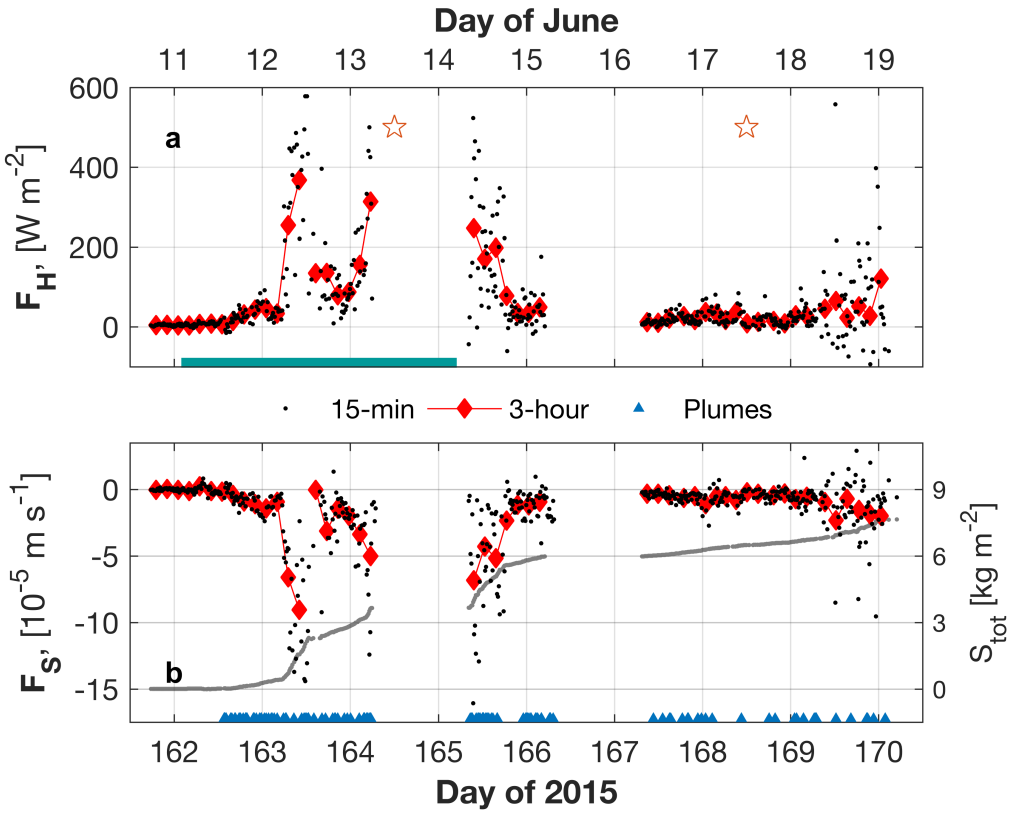

Figure 1. Turbulent fluxes of (a) heat and (b) salt are shown as 15-minute data points (dots) and 3-hour bin-averages (red). A passing storm is indicated by the green line (defined in [*Cohen et al.*]). Time of the ice cores (Figure 3) are indicated by stars. Identified plumes are indicated by blue triangles. Cumulative salt flux, S_{tot} is given in kg m^{-2} (gray).

where bad data are identified and removed systematically by statistical tests compared to artificial Gaussian data, as described in detail in *Peterson et al.* [2017]. The data gaps visible in Figure 1 are due to two corrupt data files.

Salinity is calculated from a SeaBird Electronics SBE4 conductivity cell. The dependence of salinity on both conductivity and temperature can introduce spurious salt fluxes because of difference in response time between the temperature sensor and the conductivity cell. A comparison with a fast-response micro-conductivity sensor (SBE07), showed that most of the covariance occurred at lower frequencies, and about 75% of the salinity flux was resolved by the SBE4 [*McPhee and Stanton*, 1996]. The present observations are obtained during moderate to strong forcing (5-35 cm s^{-1} drift speed), which improves response time of the conductivity cell.

Heat flux is calculated from the covariance of temperature and vertical velocity,

$$F_H = \rho_w c_p \langle w'T' \rangle, \tag{1}$$

where ρ_w is the water density and c_p is the specific heat capacity of the water, angled brackets indicate a temporal mean, and primes indicate detrended values (fluctuations about a 15-minute mean value). The heat flux is positive when warmer water is brought upward, and cold downward. Similarly, salinity flux is calculated as

$$F_S = \langle w'S' \rangle, \tag{2}$$

where F_S is positive when more saline water is brought upward, and fresher water moves down. Accumulated salt flux (units kg m^{-2}) is calculated by adding up 15-minute salt fluxes (m s^{-1}) multiplied by the segment's duration (s), using salinity in kg m^{-3}.

2.2 Plume detection

Plumes are identified in a similar manner as in the previous study from Van Mijenfjorden [*Widell et al.*, 2006]. 15-minute data segments are analyzed to find events defined as where at least five consecutive points have $w' < 0$, $S' > 1 \times 10^{-5}$ and $|w'S'|$ greater than 10^{-4} m s^{-1}, and $|w'S'|$ is more than five times the root mean square value of the 15-minute segment. A 60 second window centered on the peak $w'S'$ value is used for the mean plume ensemble. For each iteration, the 15-minute window is moved 5 minutes in order to also detect plumes otherwise falling on the edge of a window. Duplicate events are removed, leaving 131 identified plumes for the ensemble average, shown in Figure 2.

Averaging is done using a bootstrap calculation [*Emery and Thomson*, 2001], which resamples the data 1000 times to obtain an estimate of the average value occurring by chance. The mean plume and its 95% confidence interval from bootstrap calculations are shown in Figure 2. The shading represents percentiles of the data as a display of the variability between plumes.

2.3 Auxiliary data

The TIC data are supplemented by atmospheric data from a 10 m tall weather mast [*Cohen et al.*; *Hudson et al.*, 2015], and navigational data from the research vessel Lance, which was anchored to the same ice floe during the drifts, approximately 3-400 m away.

Ice cores were sampled throughout the campaign, for different ice types and sampling variables [*Granskog et al.*, 2017]. Two ice cores with both temperature and salinity measurements were collected on the same ice floe as the flux measurements, and are used in this study. Brine volume is calculated as $\Phi = S_{bu}/S_{br}$, where S_{bu} is the bulk salinity, and brine salinity is calculated using the linear fit $S_{br} = -T/0.05411$, which is adequate for warm ice [*Notz et al.*, 2005].

2.4 Data availability

The following data sets are used in this study and are publicly available at the Norwegian Polar Data Centre: Turbulence instrument cluster data [*Peterson et al.*, 2017], meteorological data [*Hudson et al.*, 2015], ice thickness from hot wires [*Rösel et al.*, 2016] and ice core data (will be made available on data.npolar.no).

3 Results

Eddy co-variance measurements from 1 m below the ice under-surface reveal anti-correlated turbulent heat and salt fluxes (Figure 1, $r = -0.94$), at a time of rapid bottom melt. Oceanic heat fluxes are directed towards the ice, and reach several hundred W m^{-2} in response to a passing storm. Salt fluxes are directed down from the ice, exceeding 10^{-4} m s^{-1}.

The observed heat- and salt fluxes imply relatively cool, saline water above warmer, fresher water, which is an inherently unstable configuration that cannot be sustained over time. Unstable conditions can occur during a frontal passage, where the observation point (ice floe) drifts from cool and saline water into an area of warmer, fresher water [*McPhee et al.*, 1987].

One possibility is if the floe drifts over an area of recent ice melt, subsequently warmed by insolation. Shear from the drifting ice could then drag the denser water over the lighter, which would immediately cause overturning of the water masses. In the present observa-

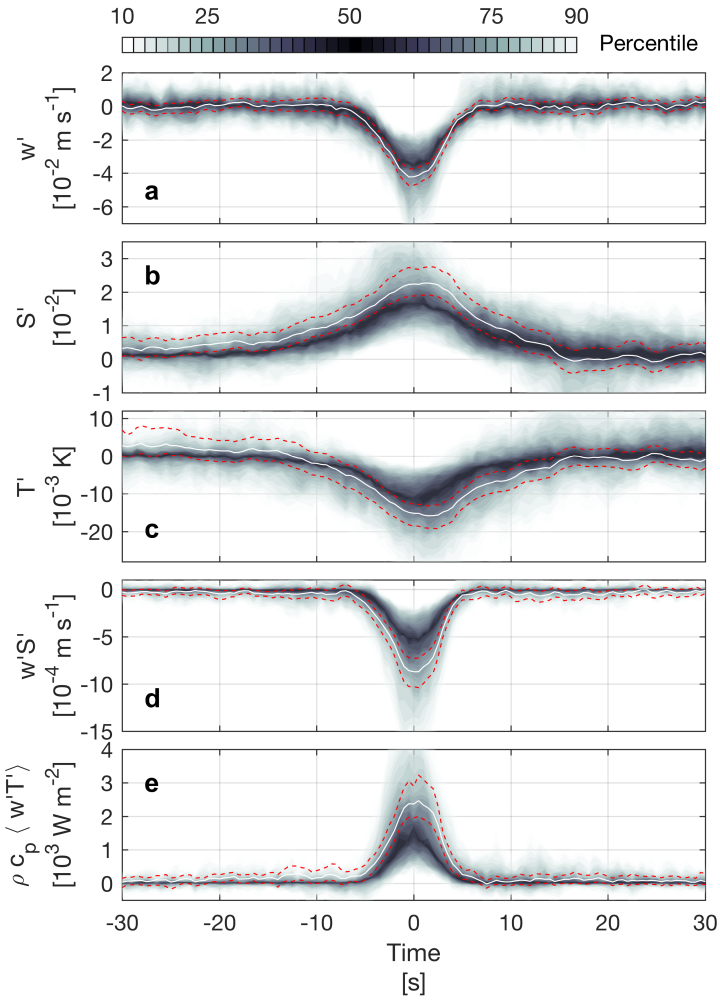

Figure 2. Composite of 131 plumes, identified using the peak in $\langle w'S' \rangle$, presented in a 60 second window. Spread in the data is shown as percentiles (shading), overlain by the mean (white) and its 95% confidence interval from bootstrap calculations (dashed red). Variables are fluctuations of (a) vertical velocity, (b) salinity (c) temperature, and turbulent fluxes of (d) salt and (e) heat.

tions, however, the negative relationship between salt and heat fluxes is sustained for hours and days, disqualifying frontal processes as a sufficient explanation.

Brine released from sea ice is another possibility, consistent with negative salt flux and positive heat flux. Resemblance to the observations in the fjord study by *Widell et al.* [2006] inspired the search for an inferred, mean plume structure. Events are identified in a similar manner (Section 2.2), and an ensemble average of the 60 s surrounding 131 identified events gives a picture of the average structure, shown in Figure 2.

Location/study	**Statistic**	**w′** [cm s^{-1}]	**S′** [10^{-3}]	**T′** [mK]	**F_S** [10^{-4} ms^{-1}]	**F_H** [W m^{-2}]
Open leads [*McPhee and Stanton*, 1996]	1-h mean				-0.15	5.9
Van Mijenfjorden [*Widell et al.*, 2006]	Plume peak	-1.6	10	-3.7	-1.5	215
Whaler's Bay [*Sirevaag*, 2009]	Mean				0.19	268
	Overall mean				-0.19	75
Yermak Plateau	Plume mean	-2.0	18	-11	-3.7	1058
	Plume peak	-4.2	23	-15.8	-8.7	2465

Table 1. Statistics of fluctuations and turbulent fluxes in the present study over the Yermak Plateau in comparison with other Arctic studies of turbulent heat and salt fluxes.

The inferred plume is approximately symmetric in time about its peak. Anomalies in temperature and salinity gradually increase toward their peak values over about 10-15 s before they decrease again at the same pace. Vertical velocity perturbations, and thus also the fluxes, increase more abruptly, reaching a peak in about 7 s, before returning to near-zero. Temperature and salinity anomalies deviate somewhat from symmetry, averaging positive (2.1×10^{-3} °C and 4.0×10^{-3}) before the plume, approaching zero after. There is, however, considerable variation between individual events, and these are just characteristics of the mean structure. Salt- and heat fluxes averaged over the 14 s surrounding the inferred plume peak are $F_S = -3.7 \times 10^{-4}$ m s^{-1} and $F_H = 1058$ W m^{-2}, respectively (See Table 1).

From an ice coring site located approximately 100 m from the measurement site [*Granskog et al.*, 2016], but on the same ice floe, two ice cores sampled on June 13 and 17 give some insight (Figure 3). The ice core on June 13 shows 110 cm thick ice, with a 30 cm snow layer on top. The ice is rather warm, with a minimum temperature of -2.5°C in the interior of the ice, increasing towards the surface (-1.3°C) and the ice-ocean interface (-1.7°C). The 'C'-shaped temperature profile is indicative of a gradual warming from above. This is confirmed by atmospheric measurements, reporting temperate conditions throughout the measurements on the floe, with temperatures ranging from -2 to +2°C at 10 m height between June 7 to 20 [*Cohen et al.*]. The snow layer was thick (~30 cm), slowing heat exchange with the ice [*Granskog et al.*, 2017].

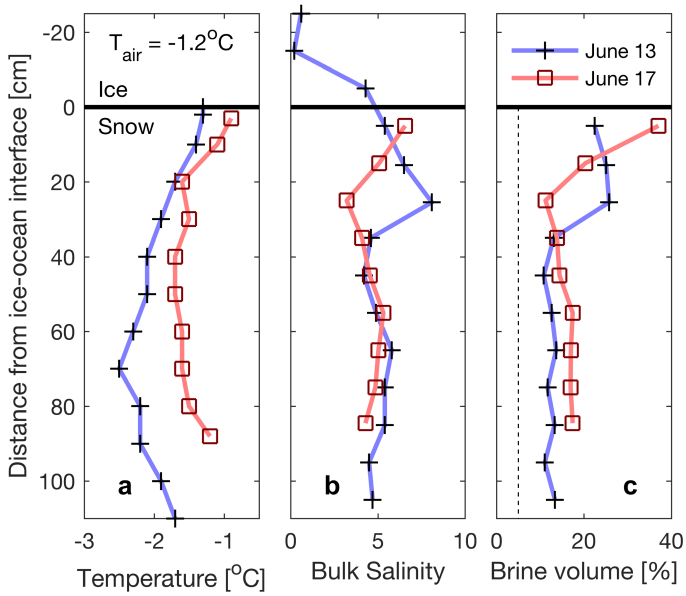

Figure 3. Vertical profiles of (a) temperature, (b) salinity and (c) brine volume fraction. The ice cores are sampled about 100 m from the measurement site on June 13 and 17. Average temperatures are -1.9 °C and °C, and bulk salinities are 6.4 and 4.8 for June 13 and 17, respectively.

Comparison of the two ice cores reveals a decrease in bulk salinity from 6.4 to 4.8, but also a change in thickness of 20 cm, together causing a change in salt content of 2.8 kg m^{-2} (calculated by multiplying bulk salinity with ice thickness). The accumulated salt release during these observations was 7.6 kg m^{-2}, summed over available measurements (Figure 1b). This is equivalent to a salinity decrease of 5 for 1.5 m thick ice. The salt flux observed here is approximately equivalent to the salt content of the June 13 ice core. About half of the salt flux was observed before the ice core was sampled, indicating that desalination had already taken place before coring. The salt flux observed after the time of coring accounts for 57% of the total salt content of the ice core on June 13. The salt flux measured between the time of the two cores is 2.8 kg m^{-2}, which corresponds very well to the change in salt content of the two ice cores. However, gaps in the time-series point to a discrepancy between ice cores and observed salt flux, which might be linked to spatial differences and variability between individual ice cores.

Calculated over the 14 s surrounding the peak salinity flux in the mean plume structure, the 131 identified events account for 0.7 m s^{-1}, or 9% of the observed total salt release, within a duration of 31 minutes (0.5% of the time), illustrating the intensity of the events.

The heat flux averaged over the composite plume is 1058 W m^{-2}, and the plumes account for 6% (4.7 W m^{-2}) of the average observed heat flux between noon June 11 until the end of measurements on June 19. However, the plumes can additionally cause mixing of the surface layers, which could counteract stabilizing effects of bottom melt. The overall effect of the plumes on heat fluxes is thus difficult to quantify. Profiles of temperature and salinity are available from these days [*Meyer et al.*, 2016], but do not provide conclusive evidence, as advection and mixed layer deepening from wind forcing obscures any effect from the plumes.

Percolation or flushing of melt ponds could influence the measurements. Although the first melt pond was noted on June 9, they remained at a very early stage throughout. The pond fraction reached an estimated 10% coverage. Mostly, ponds had formed at deformation areas where freeboard was negative, and were thus flooded with sea water rather than actual melt ponds (pers. comm., A. Rösel, January 14, 2017). From a photograph dated June 13 from the crow's nest of R/V Lance the measurement site appears unaffected by ponding (Supplemental material). The ice core from June 13 (Figure 3) had a 2 cm negative freeboard, confirmed by the high salinity (4.3) in the deepest snow layer. Based on this, and noting the high permeability of the ice (high liquid fraction, Figure 3c), percolation may have played a role in the desalination, but is not pursued further here.

The combined heat flux from above and below finally melted the sea ice. A nearby array of hot wires measuring ice thickness reveals a reduction in ice thickness of about 1 m between June 10 and June 16 (not shown) [*Rösel et al.*, 2016]. However, the thickness measurements were from a highly deformed area, and are not necessarily representative of the rest of the floe. The melt rates still agree reasonably with visual estimates at the measurement site (pers. comm., A. Meyer, 2016). At the end of the flux measurements there were only a few decimeters of ice left, and the floe disintegrated as the instruments were recovered. Over the course of the measurements, bottom melt caused an overall reduction in salinity measured at 1 m by approximately 1.

Discussion

The observations of saline plumes presented here are unprecedented. While the structure is similar to the observations from Van Mijenfjorden [*Widell et al.*, 2006], which were made with the same instrumentation on landfast ice, the magnitudes observed here are much

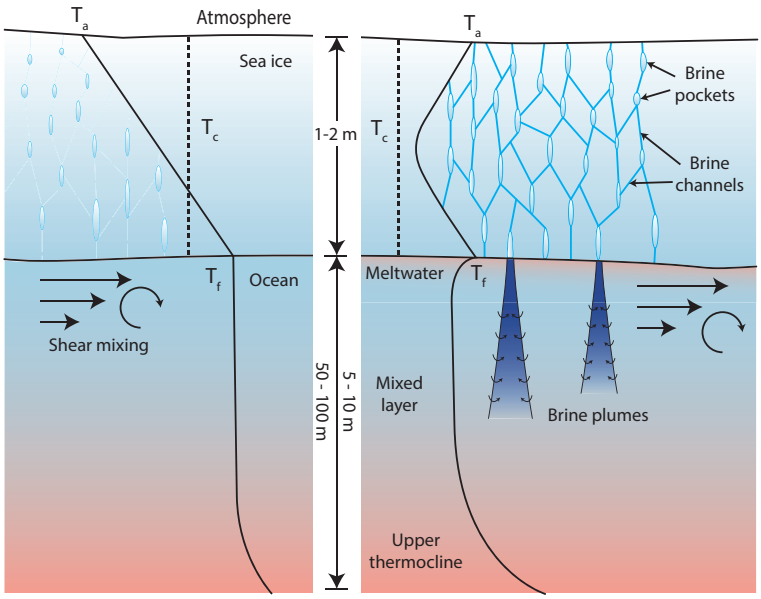

Figure 4. To the left is an early spring situation where temperature in the ice is still below the critical temperature T_c, which must be exceeded for gravity drainage to occur. When the atmosphere warms the ice, permeability of the sea ice increases, and gravity drainage can occur. The brine plumes are triggered by meltwater below the ice, elevating the freezing point temperature T_f at the interface.

greater, with peak values of salt and heat fluxes in the average plume of $F_S = -8.7\times10^{-4}$ m s^{-1} and $F_H = 2465$ W m^{-2} (See Table 1).

Gravity drainage occurs when the buoyancy of the brine exceeds the frictional forces within the sea ice. Atmospheric cooling in winter causes higher brine salinity, and thus density, higher in the ice. This makes the brine unstable, and convection within the ice will take place when the ice is sufficiently permeable [*Notz and Worster*, 2009]. As the ice warms in spring, permeability increases as illustrated in Figure 4. The brine fraction in the ice cores is > 10% throughout the ice, both well above the typical 5% threshold required for gravity drainage [*Cox and Weeks*, 1975]. The instability needed for full-depth brine convection in the ice can be triggered either by atmospheric or oceanic heat, or a combination of the two [*Griewank and Notz*, 2013]. The temperature at the ice-ocean interface is always at its salinity-determined freezing point, and warming from below can only be caused by freshening at the interface by ice melt.

Ice melts at the ocean interface when the heat supplied by the ocean exceeds the conductive heat flux in the ice. The high oceanic heat fluxes are caused by a combination of the

passing storm, presence of warm Atlantic water near the surface and the mobility of the sea ice [*Peterson et al.*, 2017; *Meyer et al.*, 2017], and accounts for much of the observed melt. As the interface freshens, the interface's salinity-determined temperature $T_f(S)$ increases. T_f remains high as long as the fresh water is allowed to remain at the interface, or enough new melt water is supplied. Additionally, fresh water supplied by melting at the ice-ocean boundary increases the density deficit between the lower part of the ice and of the brine, which may increase the potential for gravity drainage.

The hot-wire data [*Rösel et al.*, 2016] and the manual observations show that significant melt was indeed occurring, up to as much as 25 cm day^{-1} during the observation period. Furthermore, the present observations show positive temperature anomalies prior to the plume events (Figure 2c). The positive temperature anomaly before the plumes, the sustained positive heat fluxes (Figure 1a) and rapid melt suggest that oceanic heat plays a key role through ice melt, required for triggering repeated convection events.

The average mixed layer depth under the floe in June was 4.6 m [*Meyer et al.*, 2017]. If the released salt is distributed over the mixed layer it accounts for an increase in salinity of 1.7. Overall, salinity still decreases by about 1 over the course of the drift, as measured by the instrument at 1 m. The apparent inconsistency is caused by the separation in time-scales. Over longer time-scales, freshwater from ice melt is fluxed downwards, but is not apparent in the turbulence record because each 15-minute segment is detrended before fluxes are calculated. The comparison between accumulated salt flux and the salt contents of the ice core indicates that most of the brine in the ice convects down past the surface layer, rather than blending in with the fresh meltwater. Thus, it appears brine plumes as observed here affect the timing of the salt release, alter how the salt from sea ice is distributed in the water column, and can be an important factor for increased mixing during melt.

Brine drainage similar to that observed here likely occurs in the MIZ in spring in general, where enough heat is present to trigger such events. In the interior Arctic Ocean, triggering by ocean heat flux is less likely, and brine release in the quantities reported here are more likely a MIZ phenomenon. With the transition towards a more seasonal ice cover in the Arctic, the fraction of first year ice is increasing [*Meier et al.*, 2014]. First year ice is more saline [*Petrich and Eicken*, 2010], with an equivalently greater potential for brine drainage. This could indicate that saline first year ice can melt faster than fresher multi-year ice, in oth-

erwise similar conditions. Understanding desalination processes may prove to be increasingly more important in the ”new Arctic”, but will require more targeted field campaigns.

Acknowledgments

The field work has been supported by the Norwegian Polar Institute’s Centre for Ice, Climate and Ecosystems (ICE) through the N-ICE project. The author would like to thank everyone involved in the field work, and Amélie Meyer in particular, for keeping the instruments going until the very end. Thanks to Ilker Fer, Dirk Notz and Mats Granskog for useful discussions and input, and to Miles McPhee for making the instrumentation available. The author is supported by the Research Council of Norway, through the project 229786, additionally supported by from the Centre for Climate Dynamics at the Bjerknes Centre through the grant BASIC: Boundary Layers in the Arctic Atmosphere, Seas and Ice Dynamics.

References

Carmack, E. C., I. V. Polyakov, L. Padman, I. Fer, E. Hunke, J. K. Hutchings, J. Jackson, D. E. Kelley, R. Kwok, C. Layton, H. Melling, D. K. Perovich, O. Persson, B. Ruddick, M.-L. L. Timmermans, J. M. Toole, T. Ross, S. Vavrus, and P. Winsor (2015), Toward quantifying the increasing role of oceanic heat in sea ice loss in the new Arctic, *Bulletin of the American Meteorological Society*, *96*(12), 2079–2105, doi:10.1175/BAMS-D-13-00177.1.

Cohen, L., S. R. Hudson, V. P. Walden, R. M. Graham, and M. A. Granskog (), Meteorological conditions in a thinner Arctic sea ice regime from winter through spring during the Norwegian young sea ICE expedition (N-ICE2015), *Journal of Geophysical Research - Atmospheres*, p. (in revision).

Cox, G. F. N., and W. F. Weeks (1975), Brine drainage and initial salt entrapment in sodium chloride ice, *Tech. Rep. 345*, U.S. Army Cold Reg. Res. and Eng. Lab., Hanover, N. H.

Emery, W. J., and R. E. Thomson (2001), *Data analysis methods in physical oceanography*, 2 ed., 227–233 pp., Elsevier.

Golden, K. M., S. F. Ackley, and V. I. Lytle (1998), The percolation phase transition in sea Ice, *Science*, *282*(5397), 2238–2241, doi:10.1126/science.282.5397.2238.

Granskog, M. A., P. Assmy, S. Gerland, G. Spreen, H. Steen, and L. H. Smedsrud (2016), Arctic research on thin ice: Consequences of Arctic sea ice loss, *Eos*, *97*, doi:10.1029/2016EO044097.

Granskog, M. A., A. Rösel, P. A. Dodd, D. V. Divine, S. Gerland, T. Martama, and M. J. Leng (2017), Snow contribution to first-year and second-year Arctic sea ice mass balance north of Svalbard, *Journal of Geophysical Research - Oceans*, p. In press, doi: 10.1002/2016JC012398.

Griewank, P. J., and D. Notz (2013), Insights into brine dynamics and sea ice desalination from a 1-D model study of gravity drainage, *Journal of Geophysical Research: Oceans*, *118*(7), 3370–3386, doi:10.1002/jgrc.20247.

Hudson, S. R., L. Cohen, and V. Walden (2015), N-ICE2015 surface meteorology v2, doi: 10.21334/npolar.2015.056a61d1.

Jardon, F. P., F. Vivier, M. Vancoppenolle, A. Lourenço, P. Bouruet-Aubertot, and Y. Cuypers (2013), Full-depth desalination of warm sea ice, *Journal of Geophysical Research: Oceans*, *118*(1), 435–447, doi:10.1029/2012JC007962.

McPhee, M. G. (2002), Turbulent stress at the ice/ocean interface and bottom surface hydraulic roughness during the SHEBA drift, *Journal of Geophysical Research*, *107*(C10), 8037, doi:10.1029/2000JC000633.

McPhee, M. G., and T. P. Stanton (1996), Turbulence in the statically unstable oceanic boundary layer under Arctic leads, *Journal of Geophysical Research: Oceans*, *101*(C3), 6409–6428, doi:10.1029/95JC03842.

McPhee, M. G., G. A. Maykut, and J. H. Morison (1987), Dynamics and thermodynamics of the ice/upper ocean system in the marginal ice zone of the Greenland Sea, *Journal of Geophysical Research*, *92*(C7), 7017, doi:10.1029/JC092iC07p07017.

McPhee, M. G., J. H. Morison, and F. Nilsen (2008), Revisiting heat and salt exchange at the ice-ocean interface: Ocean flux and modeling considerations, *Journal of Geophysical Research - Oceans*, *113*(C6), doi:10.1029/2007JC004383.

Meier, W. N., G. K. Hovelsrud, B. E. van Oort, J. R. Key, K. M. Kovacs, C. Michel, C. Haas, M. A. Granskog, S. Gerland, D. K. Perovich, A. Makshtas, and J. D. Reist (2014), Arctic sea ice in transformation: A review of recent observed changes and impacts on biology and human activity, *Reviews of Geophysics*, *52*(3), 185–217, doi:10.1002/2013RG000431.

Meyer, A., I. Fer, A. Sundfjord, A. K. Peterson, L. H. Smedsrud, M. Muijlwick, A. Randelhoff, L. Håvik, Z. Koenig, I. Onarheim, P. Davies, J. Miguet, and N. Kusse-Tiuz (2016), N-ICE2015 ocean microstructure profiles (MSS90L), doi:10.21334/npolar.2016.774bf6ab.

Meyer, A., A. Sundfjord, I. Fer, C. Provost, N. V. Robineau, Z. Koenig, I. H. Onarheim, L. H. Smedsrud, P. Duarte, P. A. Dodd, R. M. Graham, S. Schmidtko, and H. Kauko (2017),

Winter to summer oceanographic observations in the Arctic Ocean north of Svalbard, *Journal of Geophysical Research - Oceans*, p. In press, doi:10.1002/2016JC012391.

Notz, D., and M. G. Worster (2009), Desalination processes of sea ice revisited, *Journal of Geophysical Research: Oceans*, *114*(5), 1–10, doi:10.1029/2008JC004885.

Notz, D., J. S. Wettlaufer, and M. G. Worster (2005), A non-destructive method for measuring the salinity and solid fraction of growing sea ice in situ, *Journal of Glaciology*, *51*(172), 159–166, doi:10.3189/172756505781829548.

Peterson, A. K., I. Fer, A. Randelhoff, A. Meyer, L. Håvik, L. H. Smedsrud, I. Onarheim, M. Muijlwick, A. Sundfjord, and M. G. McPhee (2016), N-ICE2015 ocean turbulent fluxes from under-ice turbulent cluster, doi:10.21334/npolar.2016.ab29f1e2.

Peterson, A. K., I. Fer, M. G. McPhee, and A. Randelhoff (2017), Turbulent Heat and Momentum Fluxes in the Upper Ocean Under Arctic Sea Ice, *Journal of Geophysical Research - Oceans*, p. In press, doi:10.1002/2016JC012283.

Petrich, C., and H. Eicken (2010), Growth, structure and properties of sea ice, in *Sea Ice*, edited by D. N. Thomas and G. S. Dieckmann, 2nd ed., chap. 2, pp. 23–77, John Wiley & Sons.

Rösel, A., M. Bratrein, J. A. King, P. Itkin, D. Divine, Å. Ervik, J.-C. Gallet, A. Gierisch, J. Haapala, A. Oikkonen, G. E. Liston, M. Nicolaus, C. M. Polashenski, G. Spreen, S. Gerland, M. A. Granskog, and D. Perovich (2016), N-ICE2015 ice thickness from hot wires, doi:10.21334/npolar.2016.263a317f.

Sirevaag, A. (2009), Turbulent exchange coefficients for the ice/ocean interface in case of rapid melting, *Geophysical Research Letters*, *36*, doi:10.1029/2008GL036587.

Turner, J. S. (2010), The melting of ice in the Arctic Ocean: The influence of double-diffusive transport of heat from below, *Journal of Physical Oceanography*, *40*(1), 249–256, doi:10.1175/2009JPO4279.1.

Widell, K., I. Fer, and P. M. Haugan (2006), Salt release from warming sea ice, *Geophysical Research Letters*, *33*(12), 1–5, doi:10.1029/2006GL026262.